Iranian Food Science and Technology Research Journal
Homepage: https://ifstrj.um.ac.ir

Research Article
Vol. 22, No. 5, Nov.- Dec. 2026, p. 449-472

The Impact of Non-thermal Technologies on the Printability and Functional Properties of Quinoa Protein-Based Food Ink

M. Sarraf[1], S. Naji-Tabasi[1*], B. Ghorani[1*], B. Emadzadeh[2], O.S. Toker[3]

1- Department of Food Nanotechnology, Research Institute of Food Science and Technology (RIFST), Mashhad, Iran
2- Department of Food Physics, Research Institute of Food Science and Technology (RIFST), Mashhad, Iran
3- Chemical and Metallurgical Faculty Food Engineering, Yildiz Technical University, Istanbul, Turkey
(*- Corresponding Authors Email: s.najitabasi@rifst.ac.ir, b.ghorani@rifst.ac.ir)

Received: 13.01.2026
Revised: 18.02.2026
Accepted: 25.02.2026
Available Online: 19.05.2026

How to cite this article:
Sarrafa, M., Naji-Tabasia, S., Ghorania, B., Emadzadehb, B., & Toker, O.S. (2026). The impact of non-thermal technologies on the printability and functional properties of quinoa protein-based food Ink. *Iranian Food Science and Technology Research Journal*, *22*(5), 449-472. https://doi.org/10.22067/ifstrj.2026.97432.1545

Abstract

In the past decade, the food industry has seen increased focus on diverse and practical designs. Accordingly, this research aims to use additive manufacturing to create gel structures from a new perspective. In this study, quinoa protein (QP), either untreated (B) or treated with cold plasma (CP) or pulsed electric fields (PEF), at two concentrations (9 and 12% w/w), was combined with polysaccharides (alginate and agar) to prepare gels. The printability and physicochemical (water activity, dry matter, water holding capacity, and color analyses), textural, and rheological properties of gels were then compared. Evaluation of the textural properties revealed that the highest hardness was observed 530.27, 416.52, and 334.82 g for the 12% B, 12% CP, and 9% PEF samples, respectively. However, in examining the results of the frequency sweep, 9% and 12% CP had the lowest storage modulus among the other gels. The 3D printing results of gels indicated that they are printable and showed high stability over 24 hr. In addition, phase separation did not occur in all treatments when gels were exposed to severe stress. Therefore, optimizing quinoa protein gels for 3D printing requires coordinating processing parameters with the composition of the formulation. This could advance the development of novel food designs with enhanced texture and stability, aligning with the food industry's focus on innovative and practical solutions.

Keywords: 3D food printing, Cold-Plasma, Hydrocolloids, Quinoa protein, Pulsed electric field

Introduction

''Three-dimensional printing'' is a rapid prototyping technology that utilizes digital model files. This technique constructs physical components or structures through the layer-by-layer deposition of materials (Godoi, Prakash, & Bhandari, 2016; Shi, Zhang, & Bhandari, 2021). In the past decade, there has been a significant increase in the demand for specialized food products tailored to specific consumer groups. This trend is especially prominent among individuals with specific nutritional requirements and personalized dietary preferences, leading to a growing demand for innovative food processing technologies that preserve desirable product properties (Godoi *et al*., 2016; Shi *et al*., 2021). Three D printing is a technology widely used in food, affecting not only the shape, taste, structure, and color of various foods but also offering potential improvements in precision, customization, and shelf life (Guo, Zhang, &

Authors retain the copyright. This is an open access article distributed under Creative Commons Attribution 4.0 International License (CC BY 4.0).
https://doi.org/10.22067/ifstrj.2026.97432.1545

Bhandari, 2019; Shi *et al*., 2021; Xiao *et al*., 2025). These materials possess a melty or mushy consistency at room temperature, enabling the creation of intricate and refined shapes through the use of Computer-Aided Design (CAD).

The most important features of the ink used in 3D printing are its ability to flow uniformly through the nozzle and to possess sufficient mechanical properties to maintain structural stability (Guo, Zhang, & Devahastin, 2020; Shi *et al*., 2021; Sun, Zhang, & Chen, 2020). Applications of this printing technology within the food industry are diverse, as demonstrated in research on chocolate (You, Huang, & Lu, 2023), Flour products (Lim, Lim, Kim, & Park, 2023; Mallesham, Parveen, Pandiselvam, Rajkumar, & Naik, 2024), Meat productions (Dong, Wang, Yang, & Xu, 2023), and gels (Shi *et al*., 2021; Yang, Zhang, Bhandari, & Liu, 2018).

In addition to the diversity of tastes, people's preferences have shifted towards healthy, nutritious and dietary foods. Therefore, the replacement of animal protein with plant proteins has also increased in consumer societies (Xiao, Zou, Hu, Zhu, & Wei, 2023; Xu *et al*., 2024).

Quinoa is regarded as one of the most exceptional plant-based resources for protein supplementation. Classified as a pseudo-cereal, it possesses protein content comparable to that of legumes. Its popularity can be attributed to its distinctive amino acid profile and its significantly higher protein content in comparison to conventional cereals (Felix, Camacho-Ocaña, López-Castejón, & Ruiz-Domínguez, 2021; Manohar, Rehman, & Sivakumaran, 2021; Pereira *et al*., 2019). Quinoa is primarily composed of globulins (37%) and albumins (35%), with a lesser proportion of prolamins (0.5–7.0%). This pseudo-cereal is noteworthy for its abundance of essential amino acids, including lysine, histidine, and methionine, which are typically limited in conventional cereal proteins (Xu *et al*., 2024). These attributes contribute significantly to its role in supporting growth and maintaining metabolic activity. Furthermore, quinoa's gluten-free nature, high antioxidant properties, substantial globulin content, and ability to form disulfide bonds underscore its potential as a valuable food ingredient in various nutritional applications (Galante, De Flaviis, Boeris, & Spelzini, 2020).

Recent studies have systematically investigated various modification approaches to enhance QP gelation properties (Farahmand *et al*., 2026). Ma *et al.* 2025 developed hybrid protein gels with complementary amino acid profiles by blending ultrasound-pretreated (100-400 W) lentil and quinoa proteins (Ma, Xiong, & Jiang, 2025). Ultrasound treatment significantly enhanced protein solubility (32% and 22% for lentil and quinoa, respectively) and gelling capacity ($p < 0.05$), yielding 1.9-fold higher gel hardness. Improved rheological properties and network density were attributed to enhanced hydrophobic and polar interactions. The resulting binary gels exhibited superior digestibility, demonstrating potential for dysphagia foods, meat analogues, and other gel-based formulations. Xu *et al.* (2024) reported that gels made from quinoa protein treated with ultrasound showed improvements for use as egg substitutes in bread (Xu *et al*., 2024). In the study by Cao *et al.* (2023), the gel strength of quinoa protein gel increased markedly by 94.12% with 600 W ultrasonic treatment, and the water-holding capacity increased from 56.6% to 68.33%. The gel solubility was reduced and free amino content led to increase the apparent viscosity and the consistency index (Cao *et al*., 2023).

Among proteins extracted from various food sources, some exhibit desirable functional properties in the food industry, while others, having undesirable functional properties, are lost as waste or byproducts. To ensure a stable supply of food protein and manage associated costs, it is essential to modify protein structures (Yang *et al*., 2025). Such modifications will enhance functional properties and significantly expand industrial applications (Nasrabadi, Doost, & Mezzenga, 2021). External factors,

for instance, oxidation effects, temperature, and pH, limit the functional properties of native proteins and restrict their application in the food industry (Wang *et al.*, 2023). Modifying the physicochemical properties of proteins by altering their structure and controlling their functional properties can be beneficial for utilizing proteins extracted from various food sources in different applications at an industrial level (Farahmand *et al.*, 2026; Wang *et al.*, 2024). Zare, Mollakhalili-Meybodi, Fallahzadeh, & Arab, (2022) systematically investigated atmospheric pressure cold plasma treatment of quinoa flour, demonstrating that treatment duration (5-20 min) and voltage (15-25 kV) significantly modified protein secondary structure. At optimal conditions (15 kV, 15 min), surface hydrophobicity increased by 47%, while disulfide bond formation enhanced by 32%. However, prolong treatment (>20 min) induced protein aggregation and decreased solubility by 28%, establishing critical processing thresholds. Ahmadian, Sohbatzadeh, Alashti, & Kenari, (2025) extended this work to protein-polysaccharide complexes, showing that surface dielectric barrier discharge plasma modified protein-polysaccharide interactions through controlled oxidation. Recently, Farahmand *et al.* (2026) provided foundational characterization of PEF-treated QP, demonstrating that 5000 V cm^{-1} with 80 pulses induced partial unfolding (α-helix content reduced from 28% to 19%) while maintaining solubility (>85%). Surface hydrophobicity increased by 62%, and free sulfhydryl groups increased by 41%, indicating controlled denaturation favorable for subsequent gelation.

From another perspective, plant proteins are often not well-suited for 3D printing, which requires modifications to make them behave like ink. This issue can be attributed to poor solubility and aggregation, weak gelation, and particularly inadequate rheological properties. Three D printing demands specific rheological characteristics. The ink must exhibit a solid-like consistency when at rest while demonstrating liquid-like flow when subjected to force, a phenomenon referred to as shear-thinning. Typically, native protein solutions lack this characteristic; therefore, modifications are essential to optimize the behavior of the proteins and achieve the necessary "extrude-and-hold" quality. Furthermore, these modifications facilitate the unfolding of the proteins, allowing them to establish a robust, elastic, self-supporting gel network that effectively retains the printed shape (Xu *et al.*, 2025).

One of these methods of modifying proteins is cold plasma (CP), which boosts the functional properties of proteins. CP is a novel, mainly untested non-thermal technology with tremendous promise for many food processing applications (Heydari *et al.*, 2023).

The pulsed electric field (PEF) technique is another non-thermal processing method that applies short bursts of high voltage to food products to electroporate cell membranes for various processing purposes. The benefits of PEF are cost-effective compared to the traditional method, less time, energy, and water consumption, and retaining the quantitative nutritional properties (Sarraf, Naji-Tabasi, & Beig-babaei, 2021).

The integration of proteins with polysaccharides facilitates the formation of thick, gel-like layers that exhibit charge characteristics (Sarraf *et al.*, 2023). Polysaccharides, like sodium alginate (SA), have properties such as biosafety, biocompatibility, and renewability (Gao *et al.*, 2020). It is a natural polysaccharide extracted from kelp or sargassum of brown algae and composed of β-D-mannuronic acid and α-L-guluronic acid (Guo, Qin, Chang, & Lee, 2023). It is challenging to use SA alone to cope with the complex water environment, as it encounters difficulty due to its poor mechanical strength, low structural stability, and low heat resistance (Ates, Koytepe, Ulu, Gurses, & Thakur, 2020).

Agar is another complex polysaccharide that is present in the cellular wall of red algae. It has a high gelling power in an aqueous solution; no need to add reagents to produce gelation and

used to improve printability. Agar also boasts remarkable reversibility when melted, and it possesses the highest natural gel strength of any gelling agent (Kim, 2014).

Until now, research has shown that QP emulsion gels can be 3D printed using various polysaccharides to deliver curcumin. One effective method involves fucoidan (FU) to improve printability and stabilize curcumin encapsulation (Zhao, Hao, Guo, Chang, & Shen, 2024, 2025). Additionally, plant-based 3D-printed dysphagia diets have been developed using pea protein isolate (PPI) with QP to enhance the essential amino acid profile, along with hydrocolloids to adjust the texture (Gu *et al*., 2025). Enhancements in printability through electrostatic complexation with polysaccharides have led to better performance of QP. Notably, high internal phase emulsions (HIPEs) stabilized by QP and carrageenan exhibit optimal geometry, smooth texture, and stability. However, the effects of non-thermal technologies on the printability and functional properties of QP-based food inks remain unexplored (Zhong, Wang, & Shen, 2024). This paper investigates the combined use of CP and PEF to modify QP as a functional ink for 3D food printing. While both plant-based proteins and 3D printing are emerging fields, this study uniquely targets QP modification and systematically compares how these non-thermal techniques influence its gelation behavior with polysaccharides. In other words, despite these advances, no previous study has systematically compared cold plasma and pulsed electric field modifications of quinoa protein for gelation and 3D printing applications. The present study addresses this gap by investigating how CP and PEF treatments at two protein concentrations (9% and 12% w/w) influence the formation of composite gels with alginate and agar, evaluating their rheological, textural, microstructural, and printability characteristics. This work uniquely contributes to understanding concentration-dependent effects of non-thermal modifications and provides a foundation for developing optimized QP-based food inks for additive manufacturing applications.

This approach offers a greener and more sustainable alternative to traditional thermal or chemical modifications for enhancing protein functionality in additive manufacturing. The paper adopts a hands-on approach, connecting 3D printing performance—such as printability and stability—with underlying microstructural, textural, and rheological properties. It highlights how controlled processes, CP and PEF, alter protein structures, affecting network formation with alginate and agar. This research offers essential insights for designing plant-based food inks, facilitating the creation of customized, nutritious printed food products.

Methods and Materials

Materials

Quinoa protein (QP) was extracted according to the procedure described elsewhere (Abugoch, Romero, Tapia, Silva, & Rivera, 2008) from Saponin-free quinoa flour (Protein content based on dry weight: 16.63%), which was purchased from Zarrin Daneh Meimeh company (Iran). Sodium alginate (SA) (Fufeng, China) and Agar (Ag) (Sigma Aldrich, Germany) were used for the preparation of gels. n-hexane and ethanol were prepared from Pars Shimi (Iran) and Taghtire-Khorasan (Iran), respectively. NaOH and HCl were purchased from Merck (Germany). All chemical products were of analytical grades. Purified deionized water was used for the solution preparation.

Extraction of Protein Quinoa (QP) from Quinoa Flour

Defatted quinoa flour was prepared by mixing n-hexane and quinoa flour (3:1) under a fume hood (24 h). The mixture was then centrifuged at 7000× g for 5 min to remove the solvent. It was repeated twice to ensure complete fat removal. Next, the collected defatted quinoa flour precipitate was dried. The extraction of quinoa protein powder was performed by solubilization at pH~9 and precipitation at pH~5. The defatted flour was suspended in water (10% (w/v), and pH~ 9 was

adjusted by NaOH (2N). The suspension was stirred at room temperature for 30 min, followed by centrifugation at 9000× g for 15 min. The collected supernatant was adjusted on pH~ 5, and then it was centrifuged at 9000× g for 20 min at 4 °C. The precipitate was suspended in water, neutralized with 2 N NaOH, and homogenized. The extract contained approximately 15% (w/v) solids. The extract was lyophilized by freeze-drier and the powder was stored in a cool, dry place (Abugoch *et al.*, 2008). The protein and moisture content were determined by the Kjeldahl method (AACC, 2000) and (AOAC, 2005), respectively.

Gels Preparation

The gels were prepared using a QP:SA:Ag in a ratio of 1:1:1 (based on pretreatment experiments). Initially, the QP mixtures, consisting of either 9 or 12 w/w%, were combined with 3% SA and subjected to heating in a circulator (Julabo, EH 19) at 85 °C for a duration of 30 min before being rapidly cooled. Subsequently, hot Ag (3 w/w %) was incorporated into the mixtures and thoroughly mixed. The six formulations performed include the following coding:

(9, 12%) B-QP: 3% SA: 3% Ag;
(9, 12%) CP-QP: 3% SA: 3% Ag;
(9, 12%) PEF-QP: 3% SA: 3% Ag.

For the preparation of gels (QP and SA), biopolymers were dispersed in deionized water for 2 h and then were left overnight for complete hydration in the refrigerator (≈5 °C).

The pulse and plasma treatment conditions were selected according to our prior optimization work that provided the best gelation properties (Farahmand *et al.*, 2026). Accordingly, quinoa protein (QP) was treated using cold plasma (CP; 40 W, 15 min) and pulsed electric field (PEF; 5000 V cm^{-1}, 80 pulses), and compared with an untreated sample (blank).

3D-Printing

The gels, used as an ink, were 3D-printed by a 3D bioprinter (VafaToos Co, Mashhad, Iran) to evaluate their potential in creating structured constructs. Printing patterns included a 20 mm x 20 mm cube with 12 layers and a 2 mm diameter nozzle. The printing speed was set to 15 $mm.s^{-1}$, 100% infill density, and the optimum printing temperature was 30 ± 3 °C.

Rheological Analysis

The evaluation of the strain and frequency sweeps of the gel inks were conducted using a rheometer (Anton Paar, Germany) featuring parallel plate geometry, with a diameter of 35 mm and a gap of 1 mm. Initially, the linear viscosity region (LVR) was determined, and an appropriate shear strain within this LVE region was selected. Strain sweep tests were conducted at a constant frequency of 1 Hz, and strain of 0.1-100% at 25 °C. The conditions used for frequency sweep included frequency of 0.1-100 $rad.s^{-1}$, temperature of 25 °C, and constant strain of 0.1%. The storage modulus (G'), loss modulus (G"), loss tangent (tan δ), and complex viscosity (η*) were obtained (Rahman *et al.*, 2020).

Microstructure

Microstructure of the selected samples were studied at 25 °C using a Field Emission Scanning Electron Microscope (FESEM; GeminiSEM 300, Germany). The freeze-dried samples received a thin coating of gold to facilitate analysis. The fractures and surfaces of the gels were assessed at magnifications of 50× and 200× (Ates *et al.*, 2020).

Physicochemical Analysis

Evaluation of Water Activity (aw)

The water activity of the gels was checked by a_w meter (LabMaster/Novasina, Swiss). The gels had to be placed in conditions without exchanging moisture with the environment. The sample was pipetted into a specialized plastic container and subsequently placed within the apparatus at a controlled temperature of 25 °C. The vapor pressure of the sample was recorded on the display once it stabilized at a constant level (Shahidi, Niazmand, Sarraf, & Shahidi, 2020).

Stability of Gel by Centrifugation Test

Centrifugal stability of gels was evaluated through centrifugation (Heidoph, Germany) at 3000 rpm for 30 min (Sarraf *et al.*, 2023). The data were analyzed using the following Eq. [1]:

$$\text{Stability (\%)} = \left(\frac{Vc}{Vt}\right)\times 100 \quad (1)$$

where V_c is the gel volume after centrifugation and V_t is the total volume of the gel (Sarraf *et al.*, 2023).

Colorimetric Analysis

The images of treatments were captured in a wooden box (45 cm above the sample and at an angle of 458 with the sample plane to give a uniform light) using a plate and a digital camera (Canon EOS 1000D, Taiwan) with a lens focal length of 35 mm. The color of gel images was evaluated using a computer (Opple, 8 W, model: MX396-Y82; 60 cm in length). Parameters L*, a* and b* of images (resolution of 300 dpi) were evaluated by the Image J software (Sarraf, Beigbabaei, & Naji-Tabasi, 2024).

Determination of FT-IR on the Optimal Gel

The functional groups of optimal gel were evaluated in powder form by a Fourier Transform Infrared Spectrometer (Thermo Nicolet AVATAR 370, USA) between wavelengths of 400 and 4,000 cm^{-1} (Ates *et al.*, 2020).

Printability Assessment

The printability of the gels printed was evaluated according to the method of Ouyang, Yao, Zhao, & Sun, (2016). To this end, the parameter associated with the gelation degree was analyzed through the measurement of the perimeter (A) and area (L) of the gels during the initial hour and after a period of one day. Additionally, the printability of the samples (Pr) was assessed in accordance with Eq. 2.

$$Pr = \frac{L^2}{16\,A} \quad (2)$$

If the *Pr* is equal to 1, the gelation conditions are ideal; also, if *Pr* < 1, the printing of under-gelled samples (those that are not fully gelled) becomes feasible. *Pr* >1, indicates irregular filaments with fractured morphology (Aina *et al.*, 2024; Ouyang *et al.*, 2016).

Also, Shape retention that indicted the ability of filaments to retain their extruded shape upon deposition without significant deformation under gravity-induced stress. It is measured based on Eq. [3] (In, Jeong, Song, & Min, 2021).

$$\text{Shape retention (\%)} = \frac{h_{24}}{h_0}\times 100 \quad (3)$$

h_{24} is height after 24hr and h_0 is initial height.

Shape fidelity (%) was determined as the ratio of the printed gel height to the designed height (20 mm) (Eq. [4]) (Gao *et al.*, 2020).

Shape fidelity (%) = (Measured Dimension / Target Dimension) × 100% (4)

Dimensional Measurement

After printing each treatment, the height of the printed gels was measured twice: at the 1st h and 24th h of production. Changes were evaluated within a day at ambient temperature and a fixed place with appropriate lighting, using a ruler to observe the treatment height changes over time (In *et al.*, 2021, with modifications).

Texture Analysis

The textural characteristics of the gels printed were studied using a texture analyzer (Stable Micro System, TA-XT Plus). The parameters of hardness, adhesiveness, apparent elastic modulus, springiness, gumminess, cohesiveness, chewiness, and consistency were determined by the TPA method at 25°C. Based on the sample characteristics and dimensions of the prepared 3D gels, a probe P/75 (England) with a diameter of 40 mm was used at a rate of 1 $mm.s^{-1}$, with a Trigger force of 3 g and 30% strain. The test conditions used were based on the type of sample (Baydin, Arntsen, Hattrem, & Draget, 2022, with modifications).

Statistical Analysis

The results were analyzed as means ± SD by a completely randomized factorial design and data were analyzed using SPSS (version 11.0)

according to ANOVA. Also, the significant difference was obtained by Duncan's multiple range test ($p \leq 0.05$). The curves were plotted using Excel software 2016. Three replications were used for technical measurements.

Results and Discussion

Rheological Properties

Study on frequency sweeps evaluation, three types of systems are defined: gels, dilute solutions, and concentrated systems (Kutz, 2019). As shown in the frequency sweep curves in Fig. 1, the storage modulus (G') values were greater than the loss modulus (G") within the specified frequency range. Additionally, the graphs for G' and G" exhibited partial frequency dependence and did not intersect. These fluids are referred to as "weak gels or structural fluids." This indicates that the structure forms an intertwined network, which remains stable even at high frequencies.

As shown in Fig. 1, the G’ and G” of the treatments increased with increasing frequency. On the other hand, G’ was higher than G” in all samples, illustrating that the elastic property dominates the viscous behavior of the gels. The lowest value was associated with 9CP and then 12CP, while the highest G’ was observed in PEF and B samples. The highest G” was contributed by 12PEF. In a comparison between the B and PEF samples in different concentrations of QP, it was determined that non-thermal technologies had a positive effect on the gel properties of the QP-AG-SA gels, whereas CP weaken the biopolymer structure of QP.

The differences in rheological properties can be explained by the distinct mechanisms of the non-thermal treatments on protein structure. PEF treatment likely induced partial unfolding of quinoa proteins, exposing hydrophobic and charged groups and promoting protein–protein and protein–polysaccharide interactions. This promoted the formation of a denser three-dimensional network within the alginate–agar matrix, which increased the storage modulus (G′) and produced a stronger elastic gel (Farahmand *et al.*, 2026). In contrast, cold plasma causes mild oxidation and rearrangement of non-covalent interactions (Zare *et al.*, 2022). Therefore, this process produced a more flexible network with lower rigidity, explaining the reduced G′ but improved flow behavior during extrusion. Therefore, CP formed softer but more extrudable gels, while PEF produced stiffer gels with higher structural strength. These structural differences are consistent with the printing behavior, where PEF samples exhibited greater resistance to flow and CP samples showed smoother extrusion. Also, Heydarian, (2024) reported that different conditions play a main role in creating cross-linking or depolymerization phenomena to modify quinoa. Zare *et al.* (2022) reported similar findings regarding the reduction in viscoelastic properties of quinoa flour after applying the CP process. They discovered that the elastic moduli of the control quinoa flour were higher than those of the quinoa flour treated with CP (Zare *et al.*, 2022).

As shown in Table 1, a comparison among parameters includes the storage modulus (G’), loss modulus (G"), loss tangent (tan δ), and complex viscosity (η^*) of gels was made at 1 Hz. Gels of B and PEF exhibited higher G' values than CP. Among the samples, G′ was highest for the 12-B and 12-PEF gels. In the CP-treated gels, the G′ of the 12% sample (1570.22 Pa) was approximately twice than the 9% sample (714.82 Pa).

A similar pattern was observed in the G" modulus at a frequency of 1 Hz. The viscous modulus B for PEF gels at both concentrations of QP exceeded 400 Pa, whereas it remained below 300 Pa for the 9% and 12% CP samples. It is evident that the concentration of QP significantly influenced the increase in the G" modulus; notably, the G" modulus for the 12-QP concentration was consistently higher than that for the 9% concentration across all experimental treatments.

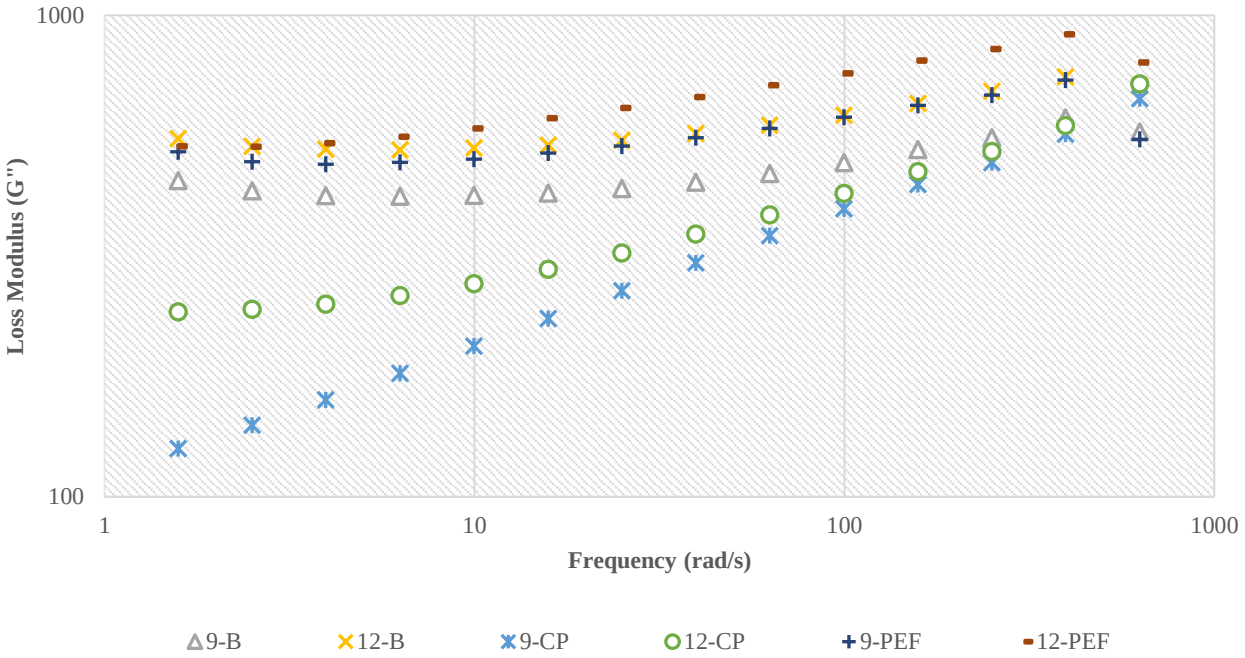

Fig. 1. Frequency sweep *(i)* G' and *(ii)* G" of gels prepared with QP (B/CP/PEF) and Ag-SA at 25°C

Table 1- Dynamic rheological parameters of gels prepared with QP (B/CP/PEF) and Ag-SA by frequency sweep test at *f*= 1 Hz and 25°C

Code	G'(Pa)	G″(Pa)	*η (Pa.s)	Tan δ
9-B	3054.90	420.39	491.03	0.14
12-B	3743.30	525.44	602.36	0.14
9-PEF	3419.4	494.84	550.16	0.14
12-PEF	3213.5	559.12	519.39	0.17
9-CP	714.82	180.46	117.39	0.25
12-CP	1570.22	261.78	253.49	0.17

The complex viscosity value (η*) of gels containing 12% B and CP showed a higher value compared to gels containing lower concentrations (9%), which indicates an increase in gel strength with the help of QP concentration, except for PEF treatments, which showed the opposite trend and increasing QP concentration caused a decrease in η*, so that, it was 550.16 and 519.39 Pa.s in 9PEF and 12PEF, respectively. The comparison of η* treatments revealed that 12-B and then PEF (9 and 12% w/w) gels exhibited stronger structures, whereas the weakest were associated with CP (Table 1).

An additional parameter for the evaluation of gels is tan δ, which quantifies the ratio of energy lost to energy stored per cycle. The tan δ value exceeding 0.1 indicates that the material may not be classified as a true gel; instead, it suggests that the structure is situated between a highly concentrated biopolymer and an actual gel (Sarraf *et al.*, 2023). Steffe's theory suggests that a tan δ value between 0.24 and 0.33 indicates a weak elastic structure in biopolymer gels, leading to the formation of amorphous polymers (Steffe, 1996). The results obtained for the treatments were in the range of 0.14-0.17, except for the 9-CP (0.25).

The rheological behavior of quinoa protein gels in this study (G' = 714-3743 Pa, tan δ =

0.14-0.25) falls within the optimal ranges established for 3D food printing across various plant protein systems. Rahman *et al.* (2020) established that successful food inks require G' between 1,000-5,000 Pa and tan δ between 0.15-0.25—criteria met by most QP formulations except 9-CP. Carranza et al. (2024) developed soy protein isolate (SPI)-alginate inks achieving optimal printability at G' values of 1,500-3,500 Pa, closely matching our 12-B (3743 Pa) and 12-PEF (3213 Pa) samples (Carranza, Tejo-Otero, Bengoechea, Guerrero, & de la Caba, 2024). The shear-thinning behavior observed across all QP gels aligns with requirements for extrusion-based printing, as documented for SPI (Carranza et al. 2024), pea protein (Jiang *et al.*, 2023), and sorghum protein (Barekat & Ubeyitogullari, 2025) systems.

Microstructural Features

The microstructural morphology of the gels prepared from three types of QP and polysaccharides was investigated using FESEM. As shown in Fig. 2, gels show a heterogeneous microstructure composed of protein-polysaccharide particles forming aggregates. According to Wang et al. (2024), proper gelation can only be achieved with suitable polysaccharide concentrations, whereas insufficient concentrations are a potential cause for failure in achieving acceptable 3D printability (Wang *et al.*, 2024). Based on Fig. 2 there are porous structures that enhance the movement of small molecules within the crystals. This phenomenon is caused by the contraction occurring through the lyophilization process (Sarraf *et al.*, 2024). Feyzmanesh, Halvaei, & Baheiraei, (2022) prepared hydrogels by alginate and according to SEM images reported that porous structures with interconnected porosities were generated in the hydrogel structures.

The application of both treated and untreated QPs significantly impacts the structural characteristics of the gels ($p \leq 0.05$). Due to their hydrophilic nature and abundance of carboxyl and hydroxyl groups presence in SA, non-covalent bonds are generated and make promote hydrophobic interactions and hydrogen bonding (Wei *et al.*, 2023; Wang *et al.*, 2024).

As demonstrated in Fig. 2 (magnifications: 50× and 200×), sample 9-B presents a rough surface that lacks a coherent network; it contains large particles, loose aggregates, and exhibits reduced compaction. A notable distinction exists between the structural appearances of samples 9-B and 12-B.

The gel with 12% QP (12-B) contained a higher density of protein aggregates embedded in the Ag-SA matrix compared to the gel with 9% QP (9-B). The network appears more crowded in 12-B. The pores in 12-B sound to be smaller but are more irregular due to the filler effect of the additional protein (Fig. 2). This aligns with the lowest hardness values observed for sample 9-B (53.10 g) and a significant increase ($p \leq 0.05$) for sample 12-B (350.27 g). This suggests that merely adding more native protein serves as a filler, enhancing resistance without necessarily forming an elegant, cohesive network, as indicated by the low cohesiveness values ranging from 0.17 to 0.22 (Table 4).

9-B

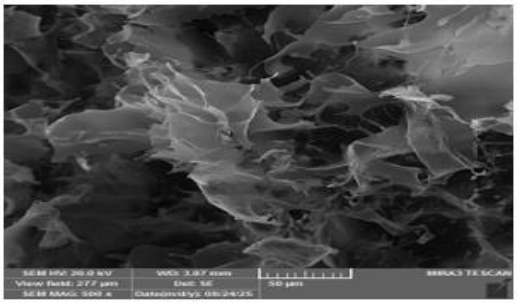

50 µm

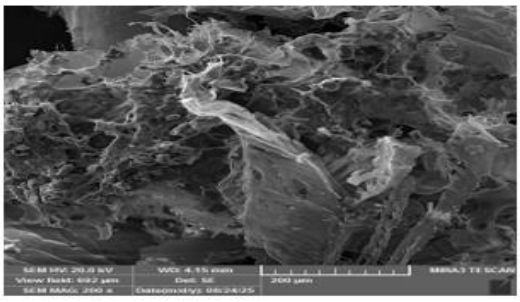

200 µm

12-B

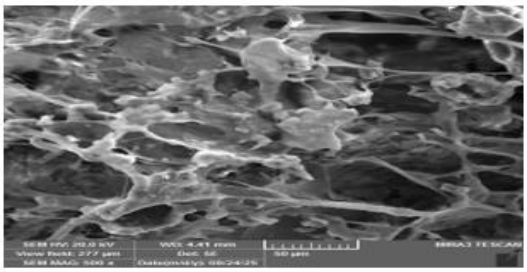

50 µm

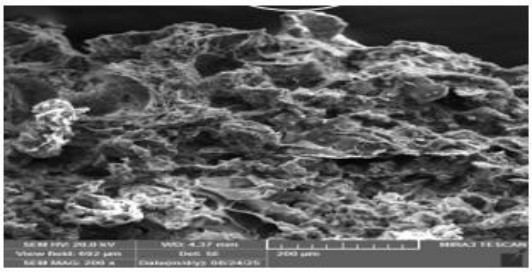

200 µm

9-PEF

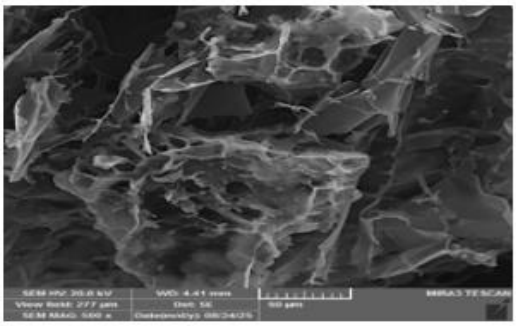

50 µm

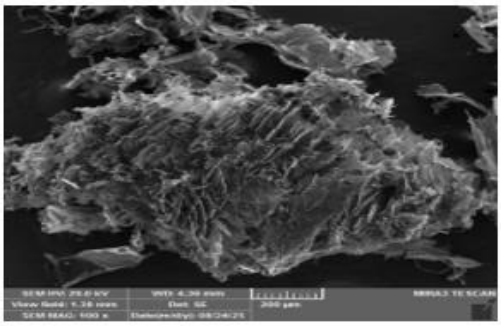

200 µm

12-PEF

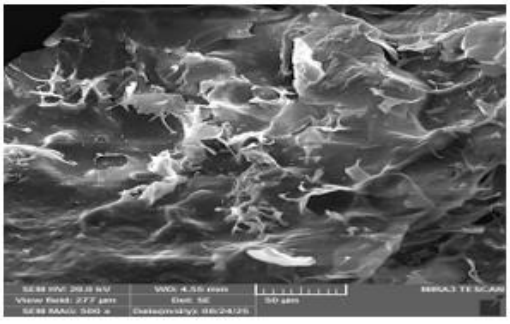

50 µm

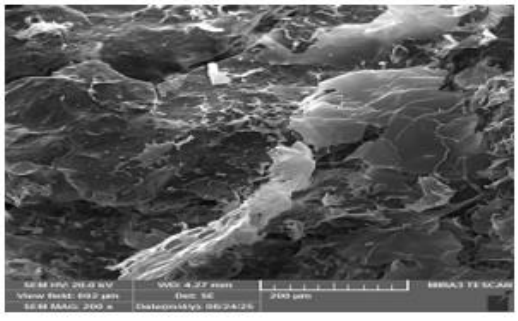

200 µm

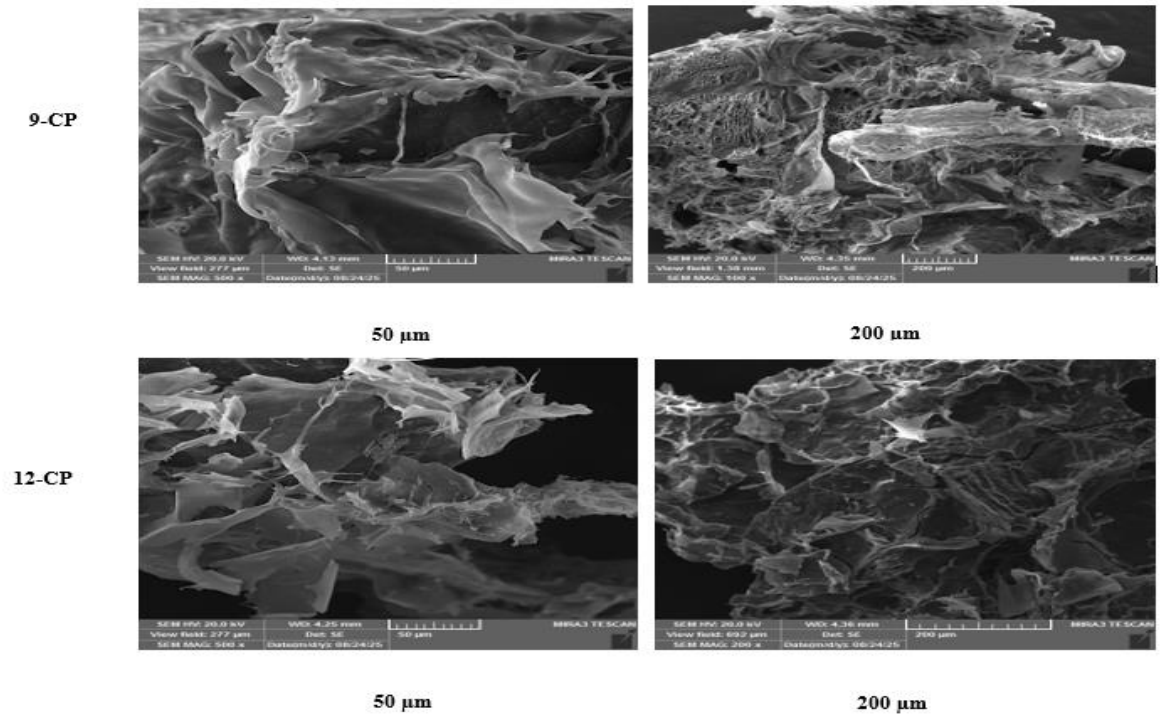

Fig. 2. The microstructural morphology (FESEM) of the gels prepared with QP (B/CP/PEF) and Ag- SA at 25 °C (50 and 100 µm)

In the 12-PEF and 9-CP images, the structure is completely heterogeneous, and roughness is observed at both magnifications. CP induces oxidation and cross-linking, creating a strong covalent protein network that integrates with Ag and SA. In light of this information, the structures of both the 9-CP and 12-CP samples exhibited a continuous and robust nature, demonstrating effective integration between the cross-linked QP and Ag-SA. This integration accounts for the elevated hardness and consistency values observed, such as the 12-CP sample, which displays a hardness of 416.52 g and a consistency of 1578.98 g·sec (Table 4). The significant cohesiveness of the 9-CP sample, with a value of 0.54, suggests that its network is not only strong but also notably balanced and resilient, resembling a highly uniform and interconnected web ($p \leq 0.05$). Conversely, the lower elasticity, indicated by G' values ranging from 714 to 1570 Pa in comparison to B/PEF gels, suggests a more rigid and less elastic microstructure (Table 1).

Similarly, PEF causes protein unfolding and electrostatic alignment without significant aggregation, promoting fine physical interactions within the matrix. Notably, the image of 9-PEF shows a somewhat uniform structure, with much less porosity and more compaction. This microstructure helps explain the high elastic modulus (G') values observed, with 9-PEF measuring 3419.4 Pa, making it the highest among all samples (Table 1). The fine, continuous network contributes to excellent elastic recovery, enabling it to store energy rather than dissipate it. The good hardness values for 9-PEF, recorded at 334.82 g, confirm that the structure is robust (Table 4). However, the lower cohesiveness compared to 9-CP indicates it may be less resistant to a second compression, likely due to the physical (non-covalent) nature of the bonds. To put it simply, the morphology of the protein-polysaccharide gels showed a more compact structure with minimal porosity compared to the protein images alone. These observations highlight the effect of non-thermal processing on protein-polysaccharide complexes, and the key role of

electrostatic interactions in determining their microstructural properties. For example, some studies reported that PEF promotes the formation of soluble protein aggregates by facilitating hydrophobic interactions among unfolded proteins (Taha *et al.*, 2023; Zhao & Yang, 2012). Also, Ahmadian et al. (2025) reported that cold plasma strengthens the interaction within the physicochemical properties of protein-polysaccharide complex that results as improve performance and increased suitability as a delivery wall material (Ahmadian *et al.*, 2025).

Physicochemical Analysis of Gels

Table 2 shows the results of water activity (a_w), dry matter (DM), water holding capacity (WHC), and color analyses of treatments. As can be seen, although a_w decreased with increasing QP percentage, no significant difference was observed among the gels. This may be attributed to the limited range of protein concentrations used and the predominance of bound water in the gel network, which buffers the effect of increased QP on the water activity.

The results of the WHC tests on the gels indicated that the samples exhibited high strength against the stress generated by the centrifugal force during centrifugation. No phase separation or water separation was observed, which suggests a strong interaction between the biopolymers (Table 2). Zare *et al.* (2022) also subjected quinoa flour to the cold plasma technique and reported that by applying the process to quinoa flour, the WHC decreased at different times and voltages (Zare *et al.*, 2022). However, the results of this study indicate that neither the CP process nor the PEF process has an adverse effect on the WHC of the gel's structure. It is worth noting that the use of QP alone has been said to create a weak structure prone to syneresis (water leakage) and poor 3D printing capability, and the addition of polysaccharides can significantly improve this structure (Zhao *et al.*, 2024). In this study, the simultaneous use of QP and polysaccharides also created a high WHC (Table 2).

Table 2- Physicochemical properties (solid materials, aw, holding capacity of water, and color parameters) of gels prepared with QP (B/CP/PEF) and Ag-SA

Code	Water Activity	Water Holding Capacity (%)	L*	a*	b*
9-B	$0.86^{a}\pm0.00$	100.00±0.00	$52.90^{a}\pm0.67$	$0.98^{e}\pm0.01$	$5.39^{e}\pm0.01$
12-B	$0.85^{ab}\pm 0.01$	100.00±0.00	$51.96^{a}\pm0.23$	$1.38^{d}\pm0.02$	$6.14^{d}\pm0.00$
9-PEF	$0.85^{ab}\pm0.00$	100.00±0.00	$45.34^{c}\pm1.12$	$1.53^{c}\pm0.02$	$6.61^{d}\pm0.02$
12-PEF	$0.84^{b}\pm0.00$	100.00±0.00	$48.46^{b}\pm0.76$	$2.61^{b}\pm0.01$	$9.18^{c}\pm0.02$
9-CP	$0.85^{ab}\pm0.01$	100.00±0.00	$41.00^{d}\pm0.10$	$4.48^{a}\pm0.01$	$11.75^{b}\pm0.00$
12-CP	$0.84^{b}\pm 0.01$	100.00±0.00	$44.53^{c}\pm0.46$	$4.50^{a}\pm0.00$	$12.40^{a}\pm0.85$

Regarding the color factor in gels, the brightness level has decreased in samples with a higher percentage of QP (12 %). On the other hand, the CP and the PEF increased the opacity of the produced protein, which in the same proportion reduced the brightness factor in the treated samples, so that the L* factor in 12% of B, PEF, and CP samples was 51.96, 48.46, and 44.53, respectively (Table 2).

Additionally, a* decreased in brightness, but expanded with protein percentage and pre-processing processes. Consequently, 12-CP exhibited the highest red spectrum and the lowest brightness among the treatments, which was also predictable from the appearance of the QP powder. Factor b* showed a trend similar to that of factor a*, with the concentration of QP and pre-treatment positively influencing this factor. Pedrali et al. (2023) noted that the factors L*, a*, and b* were observed in samples when examining various types of QP. Color pigments are predominantly located in the pericarp. Upon grinding, these pigments integrate with the lighter particles of the endosperm (Pedrali, Giupponi, De la Peña-Armada, Villanueva-Suárez, & Mateos-Aparicio, 2023).

FTIR Analysis

FTIR spectra (4000–400 cm^{-1}) of QP (untreated, CP-treated, PEF-treated) and their complexes with Ag/SA at 9% and 12% (w/w) were measured to ensure the interaction of the complex, as reported in Fig. 3.

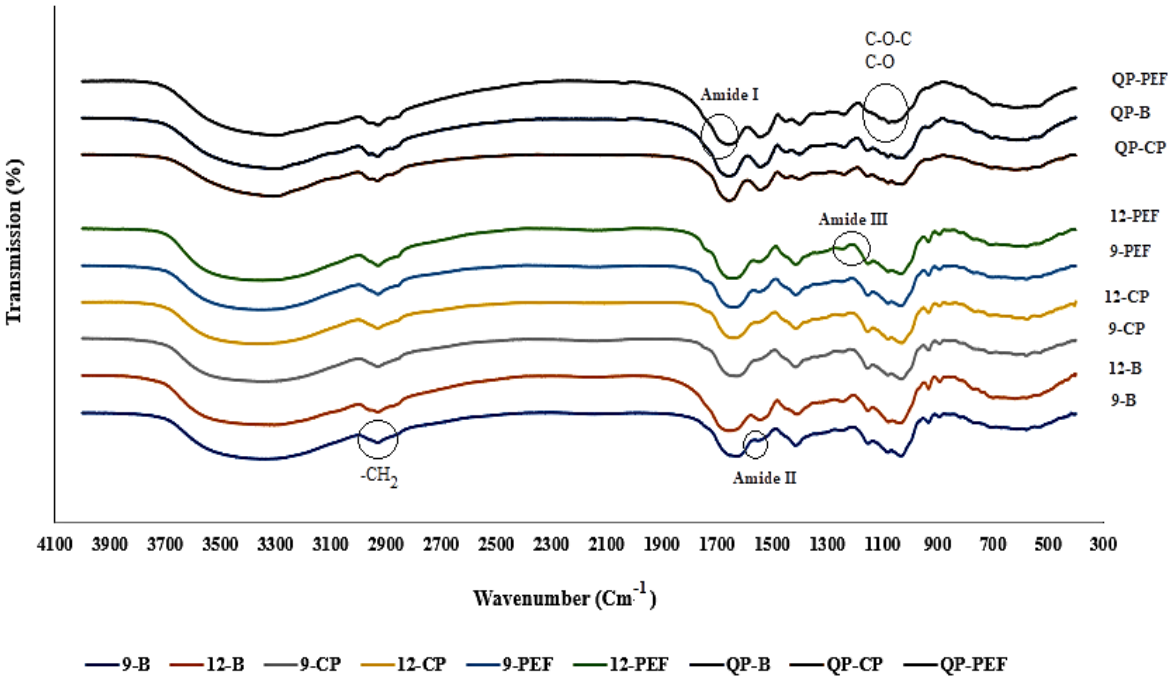

Fig. 3. FTIR spectra of dried gels prepared with QP (B/CP/PEF) and Ag-SA at 25°C

The absorption at wavenumbers of QP bands included amide I (≈1650 cm^{-1}, mainly C=O stretch), amide II (≈1540 cm^{-1}, N–H bend/C–N stretch), amide III (≈1240 cm^{-1}), and amide A (≈3300 cm^{-1}, N–H stretch). Alginate contributed symmetric/asymmetric $–COO^-$ stretches (≈1600/1400 cm^{-1}) and $–CH_2$ vibration (≈2900 cm^{-1}). (Derkach, Voron'ko, Sokolan, Kolotova, & Kuchina, 2020; Sarraf, Beig-Babaei, & Naji-Tabasi, 2021). On the other hand, the presence of the main polysaccharide structures was confirmed by a C-O-C stretching peak at 1020–1080 cm^{-1} (Derkach *et al.*, 2020).

CP and PEF samples had intensity increase and slight shifts in the wavenumbers of 1020–1080 cm^{-1} region in versus controls (9-B, 12-B). This alteration confirmed formation of hybrid QP/Ag-SA networks. The amide A band (3300–3500 cm^{-1}) broadened and shifted to lower wavenumbers in treated samples (CP > PEF > control), reflecting stronger hydrogen bonding. CP-induced oxidation enhanced cross-linking, which is reflected in the texture data, showing high hardness (Table 3) (Manzanilla-Valdez, Boesch, Martinez-Villaluenga, Montaño, & Hernández-Álvarez, 2024). While PEF promoted protein unfolding, exposing –OH/$–NH_2$ groups for elastic, homogeneous networks.

The red shift and broadening of amide I after treatment indicated a partial unfolding (α-helix → random coil), and PEF induced a slight structural disorder relative to CP. Despite the pretreatment, the main interaction peaks were consistently formed in the samples, although the intensity variations were significant. Overall, the results illustrated that hydrogen bonding are essential for the formation and stability of protein-polysaccharide complexes. Another point is about the effect of pretreatment on the interaction changes between QP and polysaccharides.

3D Printing Evaluation

Mechanism of 3D Printing

Evaluation of the 3D printability of the gels showed that all QP-polysaccharide composite

gels achieved *(i)* high-precision printing (ability to match the design model), *(ii)* high strength during printing (ability to maintain the printed form without collapsing), and *(iii)* strong structural stability over time. However treated samples showed better and more stable structures, specially pulsed treated samples.

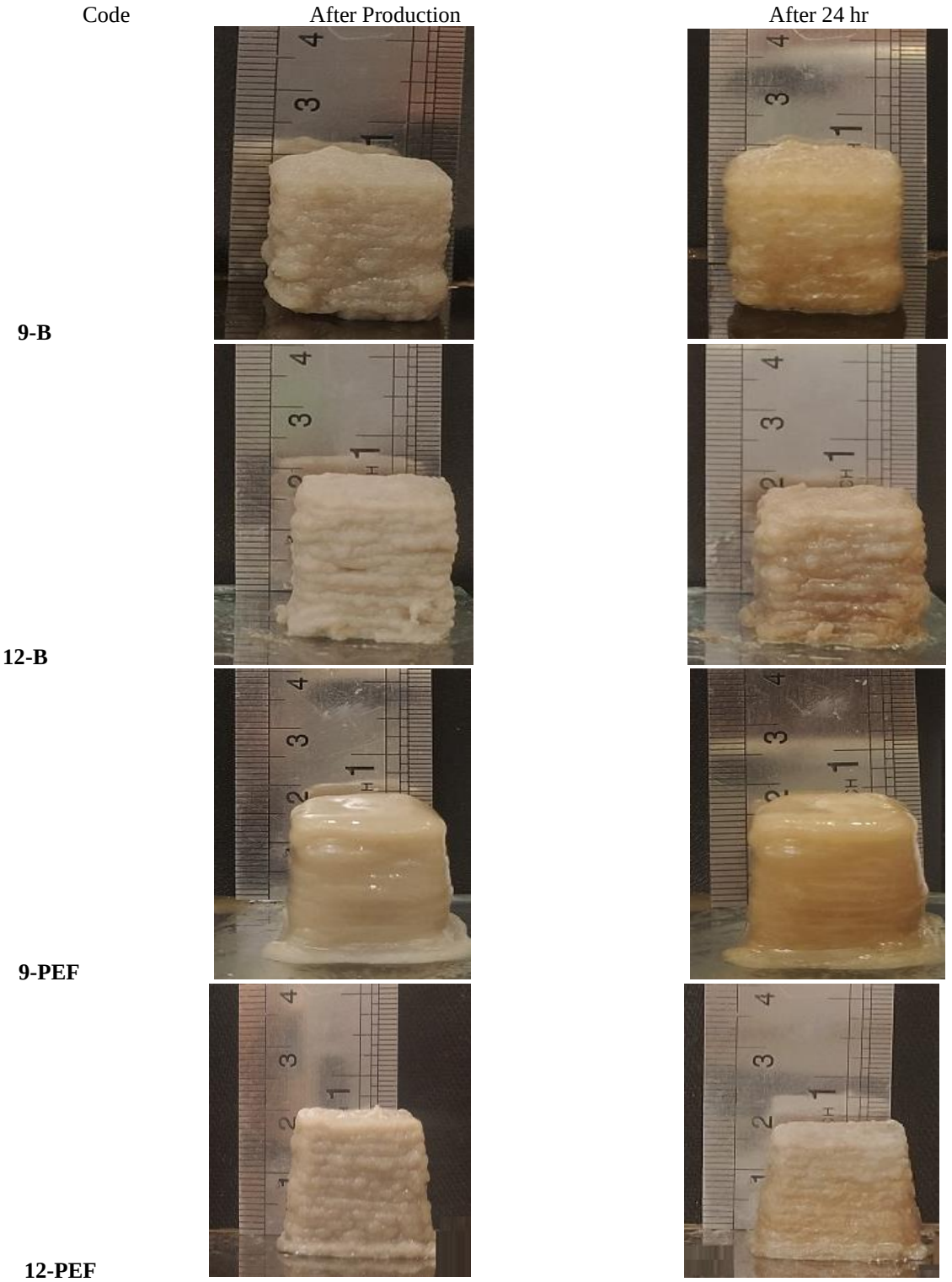

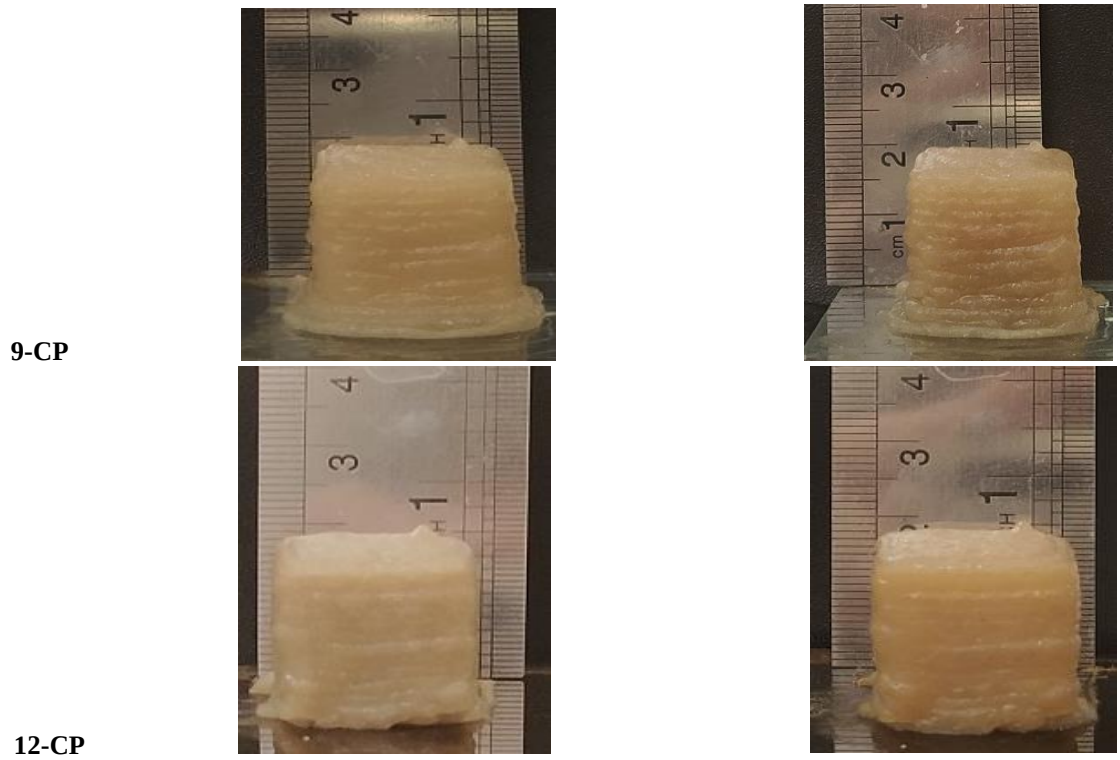

Fig. 4. 3D printability evaluation (cubic) of 3D printed gels prepared with QP (B/CP/PEF) and Ag-SA at 25 °C

On the other hand, the analysis of the rheological properties associated with the treatments reveals that all gels demonstrated shear-thinning characteristics (data not shown). This behavior indicates that, upon the application of force by the printer piston, the viscosity of the gel decreases, thus facilitating the extrusion process. It is essential to emphasize that a rapid recovery occurs during the process. Furthermore, upon completion of the process and the material's exit from the nozzle, the gel structure promptly restores its high viscose and elastic modulus (high G' and G") (Table 1). This characteristic ensures the stability of the printed layer, allowing it to bear the weight of subsequent layers effectively (Zhao *et al.*, 2024). The results were consistent across all treatments, and an evaluation of their height stability over a 24-h period showed that the productions possessed appropriate rheological properties (Fig. 4, Fig. 5).

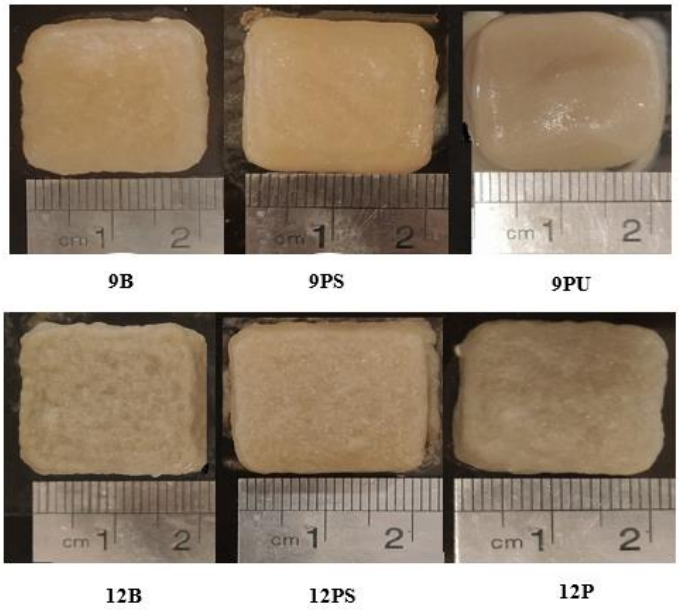

Fig. 5. Cross-section images of 3D printed gels prepared with QP (B/CP/PEF) and Ag-SA at 25 °C

Printability of 3D Printing Gels during 24 hr

The 3D printing process of the inks, as well as their dimensional measurements and the quality of appearance in additive manufacturing, were thoroughly evaluated at both 1 h and 24 h post-production (Fig. 4, Table 3).

After examining the printed gels that were stored at ambient temperature for 24 h, we observed no significant changes compared to their condition right after production ($p \leq 0.05$). This suggests that the gels have high stability and a long shelf-life. The height of the samples measured between 19.8 mm and 20 mm immediately after production, and maintained this height after 24 h. The gels exhibited strong viscoelastic behavior, and the storage modulus was high enough to maintain the ink's structure after extrusion (Zhao *et al.*, 2024).

The mechanism of this process is related to creation of cross-linking between proteins and polysaccharides, so that polysaccharides can bind to the QP (cationic) and form a dense, cross-linked network that traps water more effectively (Chen *et al.*, 2025; Chang, Gupta, Timilsena, & Adhikari, 2016). Moreover, polysaccharides can form extensive hydrogen bonds with water and proteins, while their long polymer chains intertwine with the protein network, strengthening the entire gel structure.

The printability behavior was mostly related to the structural and rheological properties of the gel inks. The samples exhibited G′ values higher than G″, which showed elastic gel behavior capable of maintaining the printed shape after extrusion. The PEF treated samples showed a more compact and continuous microstructure, which increased the storage modulus and structural strength. As a result, these samples exhibited good shape fidelity but relatively more difficult extrusion due to higher resistance to flow. Conversely, the CP treatment promoted a balanced network structure with good cohesiveness, allowing smoother extrusion while still preserving the geometry of the printed construct. The negligible change in height after 24 h confirms that the viscoelastic network was sufficiently strong to resist gravitational deformation. Therefore, printability was governed by the balance between extrusion ability (flowability) and post-printing stability (shape retention), both of which were modulated differently by CP and PEF treatments.

Table 3- Printability values and height changes (after 24h) of gels prepared with QP (B/CP/PEF) and Ag-SA at 25°C

Code	3D Printing					
	Height of the gel after formation (mm)	Height of the gel after 24 h (mm)	Printability of gel	Weight of printed gel	Shape retention (%)	Shape fidelity %
9-B	20.00^{a}±0.00	20.00 ^{a} ±0.00	1.50	6.31^{c}±0.08	100.00	100.00
12-B	19.80^{c}±0.01	19.70^{c}±0.00	1.44	7.14^{ab}±0.05	99.49	99.00
9-PEF	19.80^{c}±0.01	19.80^{b}±0.01	1.44	7.25^{ab}±0.15	100.00	99.00
12-PEF	20.00^{a}±0.00	19.80 ^{b} ±0.00	1.50	6.40^{c}±0.5	99.00	100.00
9-CP	19.90^{b}±0.00	19.80 ^{b} ±0.01	1.47	6.87^{b}±0.06	99.50	99.50
12-CP	19.80^{c}±0.01	19.80 ^{b} ±0.00	1.47	7.57^{a}±0.25	100.00	99.00

By analyzing the printability of the gels, it can be stated that the range obtained was *Pr*>1, as mentioned in section 3.8.1, which indicates excessive gelation that produces irregular filaments.

On the one hand, considering the stability over time and the retention of water under tension, and on the other hand, the high printability of these gels, the data are acceptable in response to the gels produced (Fig. 4).

The 24-h shape retention of treated/untreated QP gels (>99% for all samples) exceeds values reported for pea (85-95%) (Jiang *et al*., 2023), and soy (90-97%) (Carranza *et al*., 2024) protein systems, demonstrating exceptional structural stability of QP-Ag-SA formulations. The shape fidelity of the QP gels exceeded 99%, indicating that the printed structures closely matched the designed geometry (20 mm height) immediately after printing.

Appearance of 3D Printed Cube during Ink Extrusion

The extrusion conditions for the inks were broadly similar, except for the 12-PEF. While it demonstrated sufficient strength both during printing and over time, it felt heterogeneous to the touch, and the extrusion process was challenging. Additionally, the 9-PEF inks had a different texture and appearance compared to the 12-PEF inks (Fig. 4, Fig. 5).

The inks containing CP gels exhibited sufficient cohesion, allowing the printing process to be completed faster than the other treatments. The 9 and 12% control samples (9-B, 12-B) also showed an acceptable extrusion process and did not present any challenges. In addition, no broken filaments during printing was observed, which might be related to the smoothness effect provided by polysaccharides. In a study of Liu et al. (2018), the objects printed using xanthan- mashed potatoes and *k*-carrageenan - xanthan- mashed potatoes and the results displayed a smooth surface texture and suitable appearance due to the enhancement of soft structure and coating properties of the gum (Liu, Zhang, & Bhandari, 2018).

Texture Analysis of Gels

There are two main effective parameters on the textural properties of the gels, namely protein concentration and the type of pretreatment used on QP. The hardness parameter indicated strength of the gel structure under compression. The hardness parameter was observed to increase with QP concentration in B and CP gels. Accordingly, the highest hardness values and stiffness parameters were obtained for 12-CP and 12-B, which were 416.52 and 350.27 g, respectively. This indicated the formation of a stronger network and improved water retention compared to the gel with a lower concentration of QP. In contrast, samples of PEF exhibited reverse results, with 9-PEF showing greater hardness (Table 4).

Table 4- Textural properties of gels prepared with QP (B/CP/PEF) and Ag-SA at 25°C

Code	Hardness(g)	Adhesiveness (g.sec)	Consistency (g.sec)	Apparent elastic modulus ($g.sec^{-1}$)	Springiness (mm)	Gumminess (g)	Chewiness (g.mm)	Cohesiveness
9-B	53.10 ^{c}	-10.12^{b}	322.60^{d}	6.20^{d}	8.54^{b}	11.68^{f}	99.75^{d}	0.22^{c}
12-B	350.27^{a}	-30.79^{a}	1369.72^{b}	54.11^{b}	10.12^{a}	59.55^{d}	602.65^{c}	0.17^{d}
9-PEF	334.82^{a}	-20.48^{ab}	1298.10^{b}	66.08^{b}	8.18^{b}	97.10^{c}	794.28^{b}	0.29^{c}
12-PEF	111.10^{c}	-16.77^{ab}	607.13^{c}	18.26^{c}	8.54^{b}	14.44^{e}	123.32^{d}	0.13^{d}
9-CP	238.50^{ab}	-35.59^{a}	1216.29^{b}	56.22^{b}	8.09^{b}	128.79^{b}	1041.91^{a}	0.54^{a}
12-CP	416.52^{a}	-26.73^{ab}	1578.98^{a}	94.15^{a}	7.86^{b}	154.11^{a}	1211.30^{a}	0.37^{b}

Another important factor to be considered is adhesiveness, which measures the forces that keep a product attached to the surface of another material. The results indicate that in gels containing treated QP, adhesiveness decreased as the concentration of QP increased—conversely, the level of adhesiveness increased in gels that contain untreated QP. The consistency is another parameter and indicates the internal strength of the bonds. This characteristic showed the same results as the hardness parameter, which was predictable. The highest consistency was related to 12-B, 12-CP, and 9-PEF, which showed 1369.79, 1578.98 and 1298.10 g, respectively.

The apparent elastic modulus indicates the stiffness of the gels. Notably, the highest levels of this parameter were recorded for the samples designated as 12-B, 12-CP, and 9-PEF. Therefore, increasing the QP to 12% can have a significant effect on the hardness, stiffness and consistency of the texture in B and CP ($p \leq 0.05$). In contrast, the protein concentration of PEF poses a limitation, and the effects of this pretreatment on the network's strengthening or lack thereof should be considered.

Other parameters, such as springiness, gumminess, and chewiness, also showed an upward trend with increasing the quantities of QP. It is important to note that the texture properties of the PEF sample yielded different results; specifically, the gumminess and chewiness of the 9-PEF sample were significantly higher ($p \leq 0.05$). Chewiness in the QP pulsed samples exhibited a weak response as the concentration of QP increased; for instance, the chewiness of the 9-PEF sample measured 794.28 g.mm, while it decreased to 123.32 g.mm when the concentration of QP pulsed increased from 9% to 12%. However, in other treatments, chewiness improved with rising QP levels.

The gumminess results are completely similar to that of chewiness, and the parameter increased in B and PEF compared to CP gels, indicating a direct relationship with the chewiness characteristic.

Furthermore, the concentration of protein increased the cohesiveness of the gels, with the highest cohesiveness observed at a concentration of 9-CP. This finding indicates that while higher concentrations of QP can enhance hardness and stiffness, they negatively impact the cohesion of the texture. The results suggest an inverse relationship between the concentration of QP and cohesiveness; as the concentration increases, cohesiveness significantly decreases ($p \leq 0.05$). Therefore, high concentrations of QP did not positively influence cohesiveness and consistency.

Textural properties of QP gels (hardness: 53-416 g) span ranges comparable to optimized plant protein systems.

Textural properties of QP gels (hardness: 53-416 g) span ranges comparable to optimized plant protein systems. Xu *et al.* (2024) reported that QP gels for eggless bread achieved hardness of 425 g at 12% concentration, matching our 12-CP sample (416 g). Zhao *et al.* (2025) developed QP-fucoidan emulsion gels with hardness of 280-450 g and printability values (Pr = 1.42-1.52) almost identical to our QP-Ag-SA systems (Pr = 1.44-1.50), suggesting that Pr values of 1.4-1.5 represent a universal optimum for protein-polysaccharide composite inks.

Conclusion

This study was conducted to examine the printability, physicochemical properties, and mechanical characteristics of gels derived from QP (both treated and untreated) at concentrations of 9% and 12%, in conjunction with polysaccharides. The analysis of their rheological, textural, and printability properties revealed that one of the significant conditions to obtain optimal performance was the dependence of gel characteristics on protein concentration. In addition, the application of the non-thermal technique helped to enhance the functional properties of the gels; however, there was no statistically significant difference observed when compared to the untreated samples. Overall, optimal results were achieved by 12-B, 12-CP, and 9-PEF. This indicates that while high concentration (12%) is generally beneficial for creating firm gels, the effectiveness of novel non-thermal techniques like cold plasma and PEF is particular to the protein concentration, with PEF showing a distinct advantage at the lower 9% concentration. In future research, the use of alternative polysaccharide types, different conjugation methods, or varying process parameters could be useful to achieve the desired improvements in printability.

Acknowledgments

This work has been supported by the Center for International Scientific Studies & Collaborations (CISSC), Ministry of Science Research and Technology of Iran.

Author Contribution

Mozhdeh Sarraf: Original draft, Software, Investigation, Formal analysis, Data curation. **Sara Naji-Tabasi:** Conceptualization; Project administration; Supervision; Methodology; Validation; Review & editing. **Behrouz Ghorani:** Conceptualization; Project administration; Supervision; Methodology; Validation; Review & editing. **Bahareh Emadzadeh:** Methodology; Validation; Review & editing. **Omer Saeid Toker:** Validation; Review & editing.

Funding Source

This work has been supported by the Center for International Scientific Studies & Collaborations (CISSC), Ministry of Science Research and Technology of Iran.

Availability of data and materials

Data are available on request from the authors.

Declarations

Ethics approval and consent to participate

Not applicable.

Consent for Publication

All authors read and approved the final manuscript.

Competing Interests

The authors declare they have no competing interest.

References

1. Abugoch, L.E., Romero, N., Tapia, C.A., Silva, J., & Rivera, M. (2008). Study of some physicochemical and functional properties of quinoa (*Chenopodium quinoa* Willd) protein isolates. *Journal of Agricultural and Food Chemistry*, *56*(12), 4745–4750. https://doi.org/10.1021/jf703689u

2. Ahmadian, S., Sohbatzadeh, F., Alashti, F.J., & Kenari, R.E. (2025). Effect of surface dielectric barrier discharge plasma on the physicochemical properties of soy protein isolate-chia seed gum complex. *Food Chemistry: X*. https://doi.org/10.1016/j.fochx.2025.102574
3. Aina, M., Baillon, F., Sescousse, R., Sanchez-Ballester, N.M., Begu, S., Soulairol, I., & Sauceau, M. (2024). Evaluation of the printability of agar and hydroxypropyl methylcellulose gels as gummy formulations: Insights from rheological properties. *International Journal of Pharmaceutics*, *654*. https://doi.org/10.1016/j.ijpharm.2024.123937
4. AACC. (2000). Approved Methods of the American Association of Cereal Chemists.
5. AOAC. (2005). Official method of Analysis. 18th Edition, Association of Officiating Analytical Chemists, Washington DC, Method 935.14 and 992.24.
6. Ates, B., Koytepe, S., Ulu, A., Gurses, C., & Thakur, V.K. (2020). Chemistry, structures, and advanced applications of nanocomposites from biorenewable resources. *Chemical Reviews*, *120*(17), 9304–9362. https://doi.org/10.1021/acs.chemrev.9b00553
7. Barekat, S., & Ubeyitogullari, A. (2025). Developing hydrophobic-hydrophilic protein structures by 3D food printing of sorghum and soy protein gels. *Journal of Food Engineering*, 400, 112640. https://doi.org/10.1016/j.jfoodeng.2025.112640
8. Baydin, T., Arntsen, S.W., Hattrem, M.N., & Draget, K.I. (2022). Physical and functional properties of plant-based pre-emulsified chewable gels for the oral delivery of nutraceuticals. *Applied Food Research*, *2*(2). https://doi.org/10.1016/j.afres.2022.100225
9. Carranza, T., Tejo-Otero, A., Bengoechea, C., Guerrero, P., & de la Caba, K. (2024). Optimization of ink composition and 3D printing process to develop soy protein-based scaffolds. *Gels*, *10*(4), 223. https://doi.org/10.3390/gels10040223
10. Cao, H., Wang, X., Wang, C., Huang, K., Zhang, Y., Song, H., ... & Guan, X. (2023). Synergistic improvement of quinoa protein heat-induced gel properties treated by high-intensity ultrasound combined with transglutaminase. *Journal of the Science of Food and Agriculture*, *103*(14), 7021-7029. https://doi.org/10.1002/jsfa.12828
11. Chang, P.G., Gupta, R., Timilsena, Y.P., & Adhikari, B. (2016). Optimisation of the complex coacervation between canola protein isolate and chitosan. *Journal of Food Engineering*, *191*, 58-66. https://doi.org/10.1016/j.jfoodeng.2016.07.008
12. Chen, Q., Ji, H., Wang, Z., Wang, Y., Wang, X., & Chen, Z. (2025). Effects of different charged polysaccharides on the gelation properties and in vitro digestibility of potato protein gel: Insight into underlying mechanisms. *Food Hydrocolloids*, *164*, 111187. https://doi.org/10.1016/j.foodhyd.2025.111187
13. Derkach, S.R., Voron'ko, N.G., Sokolan, N.I., Kolotova, D.S., & Kuchina, Y.A. (2020). Interactions between gelatin and sodium alginate: UV and FTIR studies. *Journal of Dispersion Science and Technology*. https://doi.org/10.1080/01932691.2019.1611437
14. Dong, H., Wang, P., Yang, Z., & Xu, X. (2023). 3D printing based on meat materials: Challenges and opportunities. *Current Research in Food Science*, *6*. https://doi.org/10.1016/j.crfs.2022.100423
15. Farahmand, A., Naji-Tabasi, S., Ghorani, B., Emadzadeh, B., Modiri-Dovom, A., & Toker, O.S. (2026) .Pulsed electric field as a green technology for improving the structural and functional properties of quinoa protein concentrate. *Innovative Food Science and Emerging Technologies.* 104433. https://doi.org/10.1016/j.ifset.2026.104433.
16. Felix, M., Camacho-Ocaña, Z., López-Castejón, M.L., & Ruiz-Domínguez, M. (2021). Rheological properties of quinoa-based gels. An alternative for vegan diets. *Food Hydrocolloids*, *120*, 106827. https://doi.org/10.1016/j.foodhyd.2021.106827
17. Feyzmanesh, S., Halvaei, I., & Baheiraei, N. (2022). Alginate effects on human sperm parameters during freezing and thawing: a prospective study. *Cell Journal (Yakhteh)*, *24*(7), 417. https://doi.org/10.22074/cellj.2022.8122
18. Galante, M., De Flaviis, R., Boeris, V., & Spelzini, D. (2020). Effects of the enzymatic hydrolysis treatment on functional and antioxidant properties of quinoa protein acid-induced gels. *Lwt*, *118*, 108845. https://doi.org/10.1016/j.lwt.2019.108845

19. Gao, X., Guo, C., Hao, J., Zhao, Z., Long, H., & Li, M. (2020). Adsorption of heavy metal ions by sodium alginate based adsorbent-a review and new perspectives. *International Journal of Biological Macromolecules*, *164*, 4423–4434. https://doi.org/10.1016/j.ijbiomac.2020.09.046
20. Godoi, F.C., Prakash, S., & Bhandari, B.R. (2016). 3d printing technologies applied for food design: Status and prospects. *Journal of Food Engineering*, *179*, 44–54. https://doi.org/10.1016/j.jfoodeng.2016.01.025
21. Gu, H., Gu, M., Wang, Y., Wu, S., Raghavan, V., & Wang, J. (2025). Quinoa and pea protein used as a novel source producing dysphagia-oriented food by 3D printing technique. *Journal of Future Foods*. https://doi.org/10.1016/j.jfutfo.2025.07.001
22. Guo, C., Zhang, M., & Bhandari, B. (2019). Model building and slicing in food 3D printing processes: a review. *Comprehensive Reviews in Food Science and Food Safety*, *18*(4), 1052–1069. https://doi.org/10.1111/1541-4337.12443
23. Guo, C., Zhang, M., & Devahastin, S. (2020). 3D extrusion-based printability evaluation of selected cereal grains by computational fluid dynamic simulation. *Journal of Food Engineering*, *286*, 110113. https://doi.org/10.1016/j.jfoodeng.2020.110113
24. Guo, H., Qin, Q., Chang, J.-S., & Lee, D.-J. (2023). Modified alginate materials for wastewater treatment: Application prospects. *Bioresource technology*, *387*, 129639. https://doi.org/10.1016/j.biortech.2023.129639
25. Heydari, M., Carbone, K., Gervasi, F., Parandi, E., Rouhi, M., Rostami, O., Abedi-Firoozjah, R., Kolahdouz-Nasiri, A., Garavand, F., & Mohammadi, R. (2023). Cold plasma-assisted extraction of phytochemicals: A review. *Foods*, *12*(17), 3181. https://doi.org/10.3390/foods12173181
26. Heydarian, A. (2024). The significant effect of cold plasma on the modification of the characteristics of cereal starches. *Journal of Food Science & Technology (2008-8787)*, *20*(144). https://doi.org/10.22034/FSCT.20.144.25
27. In, J., Jeong, H., Song, S., & Min, S.C. (2021). Determination of material requirements for 3D gel food printing using a fused deposition modeling 3D printer. *Foods*, *10*(10), 2272. https://doi.org/10.3390/foods10102272
28. Jiang, W., Li, W., Li, J., McClements, D.J., Ma, C., Chen, S., ... & Liu, F. (2023). High internal phase emulsions stabilized by pea protein isolate-inulin conjugates: Application as edible inks for 3D printing. *Food Hydrocolloids*, *142*, 108820. https://doi.org/10.1016/j.foodhyd.2023.108820
29. Kim, S.-K. (2014). *Marine carbohydrates: fundamentals and applications, part B* (Vol. 73). Academic Press. https://doi.org/10.3390/foods10102272
30. Kutz, M. (2019). *Handbook of farm, dairy and food machinery engineering*. Academic Press.
31. Lim, W.S., Lim, N., Kim, H.W., & Park, H.J. (2023). Effect of emulsion gel as butter substitute on the dimensional stability and nutritional profile of 3D Printed Cookies. *Food Bioscience*, *56*, 103207. https://doi.org/10.1016/j.fbio.2023.103207
32. Liu, Z., Zhang, M., & Bhandari, B. (2018). Effect of gums on the rheological, microstructural and extrusion printing characteristics of mashed potatoes. *International Journal of Biological Macromolecules*, *117*, 1179-1187. https://doi:10.1016/j.ijbiomac.2018.06.048
33. Ma, Y., Xiong, Y.L., & Jiang, J. (2025). Ultrasound-enhanced reconstruction and gelation of binary lentil–quinoa protein matrix for nutrition complementary soft gels. *Food Bioscience*, *66*, 106311. https://doi.org/10.1016/j.fbio.2025.106311
34. Mallesham, P., Parveen, S., Pandiselvam, R., Rajkumar, P., & Naik, R. (2024). Characterisation of 3D printing cake batter with xanthan gum and optimization of printing parameters using response surface methodology. *International Journal of Gastronomy and Food Science*, *38*, 101026. https://doi.org/10.1016/j.ijgfs.2024.101026
35. Manohar, S., Rehman, V., & Sivakumaran, B. (2021). Role of unfamiliarity and information on consumers' willingness to try new healthy foods. *Food Quality and Preference*, *87*, 104037. https://doi.org/10.1016/j.foodqual.2020.104037
36. Manzanilla-Valdez, M.L., Boesch, C., Martinez-Villaluenga, C., Montaño, S., & Hernández-Álvarez, A.J. (2024). Enhancing quinoa (*Chenopodium quinoa* Willd) protein extraction: Alkaline solubilization

coupled to isoelectric precipitation effects on structure, digestibility and antinutrients. *Food Hydrocolloids for Health*, *6*, 100191. https://doi.org/10.1016/j.fhfh.2024.100191
37. Nasrabadi, M.N., Doost, A.S., & Mezzenga, R. (2021). Modification approaches of plant-based proteins to improve their techno-functionality and use in food products. *Food Hydrocolloids*, *118*, 106789. https://doi.org/10.1016/j.foodhyd.2021.106789
38. Ouyang, L., Yao, R., Zhao, Y., & Sun, W. (2016). Effect of bioink properties on printability and cell viability for 3D bioplotting of embryonic stem cells. *Biofabrication*, *8*(3), 035020. https://doi.org/10.1088/1758-5090/8/3/035020
39. Pedrali, D., Giupponi, L., De la Peña-Armada, R., Villanueva-Suárez, M.J., & Mateos-Aparicio, I. (2023). The quinoa variety influences the nutritional and antioxidant profile rather than the geographic factors. *Food Chemistry*, *402*, 133531. https://doi.org/10.1016/j.foodchem.2022.133531
40. Pereira, E., Encina-Zelada, C., Barros, L., Gonzales-Barron, U., Cadavez, V., & Ferreira, I.C. (2019). Chemical and nutritional characterization of *Chenopodium quinoa* Willd (quinoa) grains: A good alternative to nutritious food. *Food Chemistry*, *280*, 110–114. https://doi.org/10.1016/j.foodchem.2018.12.068
41. Rahman, J.M.H., Shiblee, M.N.I., Ahmed, K., Khosla, A., Kawakami, M., & Furukawa, H. (2020). Rheological and mechanical properties of edible gel materials for 3D food printing technology. *Heliyon*, *6*(12). https://doi.org/10.1016/j.heliyon.2020.e05859
42. Sarraf, M., Beig-Babaei, A., & Naji-Tabasi, S. (2021). Optimizing extraction of berberine and antioxidant compounds from barberry by maceration and pulsed electric field-assisted methods. *Journal of Berry Research*, *11*(1), 133–149. https://doi.org/10.3233/JBR-200603
43. Sarraf, M., Beig-babaei, A., & Naji-Tabasi, S. (2024). Edible oleogels for oral delivery of berberine in dairy food: In-vitro digestion study. *Food Science & Nutrition*, *12*(5), 3273–3281. https://doi.org/10.1002/fsn3.3994
44. Sarraf, M., Naji-Tabasi, S., & Beig-babaei, A. (2021). Influence of calcium chloride and pH on soluble complex of whey protein-basil seed gum and xanthan gum. *Food Science & Nutrition*, *9*(12), 6728–6736. https://doi.org/10.1002/fsn3.2624
45. Sarraf, M., Naji-Tabasi, S., Beig-Babaei, A., Moros, J.E., Carrillo, M.C.S., & Tenorio-Alfonso, A. (2024). Developing edible oleogels structure prepared with emulsion-template approach based on soluble biopolymer complex. *Food Chemistry: X*, *24*, 101917. https://doi.org/10.1016/j.fochx.2024.101917
46. Sarraf, M., Naji-Tabasi, S., Beig-Babaei, A., Moros, J.E., Sánchez, M.C., Franco, J.M., & Tenorio-Alfonso, A. (2023). Improving the structure and properties of whey protein emulsion gel using soluble interactions with xanthan and basil seed gum. *Food Science & Nutrition*, *11*(11), 6907–6919. https://doi.org/10.1002/fsn3.3598
47. Shahidi, N.M., Niazmand, R., Sarraf, M., & Shahidi, M. (2020). Investigation of the effect of different types of emulsifiers on the water activity and stability of walnut butter during the shelf-life. https://doi.org/10.52547/fsct.17.100.177
48. Shi, Y., Zhang, M., & Bhandari, B. (2021). Effect of addition of beeswax based oleogel on 3D printing of potato starch-protein system. *Food Structure*, *27*, 100176. https://doi.org/10.1016/j.foostr.2021.100176
49. Steffe, J.F. (1996). *Rheological methods in food process engineering*. Freeman press.
50. Sun, Y., Zhang, M., & Chen, H. (2020). LF-NMR intelligent evaluation of rheology and printability for 3D printing of cookie dough pretreated by microwave. *Lwt*, *132*, 109752. https://doi.org/10.1016/j.lwt.2020.109752
51. Taha, A., Casanova, F., Talaikis, M., Stankevič, V., Žurauskienė, N., Šimonis, P., Pakštas, V., Jurkūnas, M., Gomaa, M.A., & Stirkė, A. (2023). Effects of pulsed electric field on the physicochemical and structural properties of micellar casein. *Polymers*, *15*(15), 3311. https://doi.org/10.3390/polym15153311.
52. Wang, J., Jiang, Q., Huang, Z., Muhammad, A.H., Gharsallaoui, A., Cai, M., Yang, K., & Sun, P. (2024). Rheological and mechanical behavior of soy protein-polysaccharide composite paste for extrusion-based 3D food printing: Effects of type and concentration of polysaccharides. *Food Hydrocolloids*, *153*, 109942. https://doi.org/10.1016/j.foodhyd.2024.109942

53. Wang, R., Wang, L.-H., Wen, Q.-H., He, F., Xu, F.-Y., Chen, B.-R., & Zeng, X.-A. (2023). Combination of pulsed electric field and pH shifting improves the solubility, emulsifying, foaming of commercial soy protein isolate. *Food Hydrocolloids*, *134*, 108049. https://doi.org/10.1016/j.foodhyd.2022.108049
54. Wei, Q., Zhou, J., An, Y., Li, M., Zhang, J., & Yang, S. (2023). Modification, 3D printing process and application of sodium alginate based hydrogels in soft tissue engineering: A review. *International Journal of Biological Macromolecules*, *232*, 123450. https://doi.org/10.1016/j.ijbiomac.2023.123450
55. Xiao, S., Yang, J., Bi, Y., Li, Y., Cao, Y., Zhou, M., Pang, G., Dong, X., & Tong, Q. (2025). Food 3D Printing Equipment and Innovation: Precision Meets Edibility. *Foods*, *14*(12), 2066. https://doi.org/10.3390/foods14122066
56. Xiao, X., Zou, P.-R., Hu, F., Zhu, W., & Wei, Z.-J. (2023). Updates on plant-based protein products as an alternative to animal protein: Technology, properties, and their health benefits. *Molecules*, *28*(10), 4016. https://doi.org/10.3390/molecules28104016
57. Xu, Q., Zhang, X., Zuo, Z., Zhang, M., Li, T., & Wang, L. (2024). The preparation and characterization of quinoa protein gels and application in eggless bread. *Foods*, *13*(8), 1271. https://doi.org/10.3390/foods13081271
58. Xu, Y., Zhao, J., Zhang, M., Sun, Y., Li, X., Gao, K., & Liang, J. (2025). *Naematelia aurantialba* polysaccharide: Enhancing 3D printability of soy protein gel via rheology and interactions improvement. *International Journal of Biological Macromolecules*, 145415. https://doi.org/10.1016/j.ijbiomac.2025.145415
59. Yang, F., Zhang, M., Bhandari, B., & Liu, Y. (2018). Investigation on lemon juice gel as food material for 3D printing and optimization of printing parameters. *Lwt*, *87*, 67–76. https://doi.org/10.1016/j.lwt.2017.08.054
60. You, S., Huang, Q., & Lu, X. (2023). Development of fat-reduced 3D printed chocolate by substituting cocoa butter with water-in-oil emulsions. *Food Hydrocolloids*, *135*, 108114. https://doi.org/10.1016/j.foodhyd.2022.108114
61. Zare, L., Mollakhalili-Meybodi, N., Fallahzadeh, H., & Arab, M. (2022). Effect of atmospheric pressure cold plasma (ACP) treatment on the technological characteristics of quinoa flour. *Lwt*, *155*, 112898. https://doi.org/10.1016/j.lwt.2021.112898
62. Zhao, K., Hao, Y., Guo, X., Chang, Y., & Shen, X. (2024). Development, characterization and underling mechanism of 3D printable quinoa protein emulsion gels by incorporating of different polysaccharides for curcumin delivery. *International Journal of Biological Macromolecules*, *280*, 135648. https://doi.org/10.1016/j.ijbiomac.2024.135648
63. Zhao, K., Hao, Y., Guo, X., Chang, Y., & Shen, X. (2025). Development and characterization of quinoa protein-fucoidan emulsion gels with excellent rheological properties for 3D printing and curcumin encapsulation stability. *Food Chemistry*, *471*, 142819. https://doi.org/10.1016/j.foodchem.2025.142819
64. Zhao, W., & Yang, R. (2012). Pulsed electric field induced aggregation of food proteins: Ovalbumin and bovine serum albumin. *Food and Bioprocess Technology*, *5*(5), 1706-1714. https://doi.org/10.1007/s11947-010-0464-8
65. Zhong, W., Wang, Q., & Shen, X. (2024). Quinoa protein/polysaccharide electrostatic complex stabilized vegan high internal phase emulsions for 3D printing: Role of complex state and gelling-type polysaccharides. *Food Chemistry*, *434*, 137447. https://doi.org/10.1016/j.foodchem.2023.137447

نشریه پژوهشهای علوم و صنایع غذایی ایران
https://ifstrj.um.ac.ir

مقاله پژوهشی
جلد ۲۲، شماره ۵، آذر- دی ۱۴۰۵، ص. ۴۷۲-۴۴۹

تأثیر روش‌های غیرحرارتی بر قابلیت چاپ و خواص عملکردی جوهر غذایی مبتنی بر پروتئین کینوا

مژده صراف[۱]- سارا ناجی طبسی[۱*]- بهروز قرآنی[۱*]- بهاره عمادزاده[۲]- عمرسعید توکر[۳]

تاریخ دریافت: ۱۴۰۴/۱۰/۲۳
تاریخ پذیرش: ۱۴۰۴/۱۲/۰۶

چکیده

در دهه گذشته، صنعت غذا شاهد تمرکز فزاینده‌ای بر روی طرح‌های متنوع و کاربردی بوده است. بر همین اساس، این تحقیق با هدف استفاده از تولید افزایشی برای ایجاد ساختارهای ژل از منظری جدید انجام شده است. در این مطالعه، پروتئین کینوا (QP)، چه بدون تیمار (B) و چه تحت تیمار با پلاسمای سرد (CP) یا میدان‌های الکتریکی پالس (PEF)، در دو غلظت (۹ و ۱۲ درصد وزنی/وزنی)، با پلی‌ساکاریدها (آلژینات و آگار) ترکیب شد تا ژل‌ها تهیه شوند. سپس قابلیت چاپ و خواص فیزیکوشیمیایی (فعالیت آبی، ماده خشک، ظرفیت نگهداری آب و آنالیز رنگ)، خواص بافتی و رئولوژیکی ژل‌ها مورد بررسی قرار گرفت. ارزیابی خصوصیات بافتی نشان داد که بالاترین میزان سختی مربوط به نمونه‌های ۱۲ درصد B (۵۳۰/۲۷ g)، ۱۲ درصد CP (۴۱۶/۵۲ g) و ۹ درصد PEF (۳۳۴/۸۲ g) می‌باشد. با این حال، در بررسی نتایج فرکانس متغیر، نمونه ۹ و ۱۲ درصد CP کمترین مدول ذخیره را در بین سایر ژل‌ها نشان داد. نتایج چاپ سه‌بعدی ژل‌ها، قابلیت چاپ و پایداری بالا در طول ۲۴ ساعت در دمای محیط را نشان داد. علاوه بر این، جداسازی فازی در معرض تنش شدید در هیچ یک از تیمارها رخ نداد. بنابراین، بهینه‌سازی ژل‌های پروتئین کینوا برای فرآیند چاپ سه‌بعدی نیاز به هماهنگی پارامترهای پردازش با ترکیب فرمولاسیون دارد. این امر می‌تواند طراحی های غذایی نوین همراه با ارتقای بافت و پایداری را توسعه داده و با تمرکز صنعت غذا بر راه حل‌های نوآورانه و عملی همسو باشد.

واژه‌های کلیدی: پروتئین کینوا، پلاسمای سرد، چاپ سه بعدی محصولات غذایی، میدان الکتریکی پالس، هیدروکلوئید

۱- گروه نانوفناوری مواد غذایی، مؤسسه پژوهشی علوم و صنایع غذایی، مشهد، ایران
(*- نویسندگان مسئول: Email: b.ghorani@rifst.ac.ir; Email: s.najitabasi@rifst.ac.ir)
۲- گروه فیزیک مواد غذایی، مؤسسه پژوهشی علوم و صنایع غذایی، مشهد، ایران
۳- دانشکده شیمی و متالورژی، مهندسی مواد غذایی، دانشگاه فنی یبلدیز، استانبول، ترکیه

https://doi.org/10.22067/ifstrj.2026.97432.1545